Thermodynamic Analysis of the Lipopolysaccharide-Dependent Resistance of Gram-Negative Bacteria against Polymyxin B

Jörg Howe,* Jörg Andrä,* Raquel Conde,† Maite Iriarte,† Patrick Garidel,‡ Michel H. J. Koch,§ Thomas Gutsmann,* Ignacio Moriyón,† and Klaus Brandenburg*

*Forschungszentrum Borstel, Leibniz-Zentrum für Medizin und Biowissenschaften, D-23845 Borstel, Germany; †Universidad de Navarra, Departmento de Microbiologia, E-31008 Pamplona, Spain; ‡Institut für Physikalische Chemie, Martin-Luther-Universität Halle-Wittenberg, D-06108 Halle, Germany; and §European Molecular Biology Laboratory c/o DESY, D-22603 Hamburg, Germany

ABSTRACT Cationic antimicrobial cationic peptides (CAMP) have been found in recent years to play a decisive role in hosts' defense against microbial infection. They have also been investigated as a new therapeutic tool, necessary in particular due to the increasing resistance of microbiological populations to antibiotics. The structural basis of the activity of CAMPs has only partly been elucidated and may comprise quite different mechanism at the site of the bacterial cell membranes or in their cytoplasm. Polymyxin B (PMB) is a CAMP which is effective in particular against Gram-negative bacteria and has been well studied with the aim to understand its interaction with the outer membrane or isolated membrane components such as lipopolysaccharide (LPS) and to define the mechanism by which the peptides kill bacteria or neutralize LPS. Since PMB resistance of bacteria is a long-known phenomenon and is attributed to structural changes in the LPS moiety of the respective bacteria, we have performed a thermodynamic and biophysical analysis to get insights into the mechanisms of various LPS/PMB interactions in comparison to LPS from sensitive strains. In isothermal titration calorimetric (ITC) experiments considerable differences of PMB binding to sensitive and resistant LPS were found. For sensitive LPS the endothermic enthalpy change in the gel phase of the hydrocarbon chains converts into an exothermic reaction in the liquid crystalline phase. In contrast, for resistant LPS the binding enthalpy change remains endothermic in both phases. As infrared data show, these differences can be explained by steric changes in the headgroup region of the respective LPS.

INTRODUCTION

An important challenge in clinical care is the emergence of increasing antimicrobial resistance in bacteria. Several species are known which exhibit a pronounced resistance against the cationic antimicrobial peptide (CAMP) polymyxin B (PMB), for example. These include the deep rough mutant strain R45 from *Proteus mirabilis* and nonenterobacterial strains such as those from *Brucella abortus* (1,2). It could be shown for *P. mirabilis* Re45 that the resistance of the bacteria is directly connected with a change of the chemical structure the hydrophilic sugar part of the lipopolysaccharide (LPS), in particular the higher content of positively charged arabinose in the headgroup region of LPS (3). Bacterial LPS, also called endotoxin, is exclusively located in the outer leaflet of the outer membrane of Gram-negative bacteria and belongs to the most potent triggers of the human innate immune system. In human mononuclear cells or in macrophages, proinflammatory cytokines such as interleukins and tumor necrosis factor α are already secreted at LPS concentrations below 100 pg/ml (4). In the case of high LPS concentrations in blood, the septic shock syndrome occurs which belongs to one of the most frequent causes of mortality in hospitalized patients in critical care units. One of the reasons for this high mortality may lie in the fact that many conventional antibiotics are able to kill the bacteria, which consequently may lead to a release of LPS, but are not able to bind and neutralize LPS (5). Therefore, in recent years several approaches have been made to develop compounds, in particular antimicrobial peptides, which can neutralize bacterial endotoxins (6–9). To this group belongs the decapeptide PMB, which may effectively kill bacteria as well as neutralize free LPS (10,11). Direct application of PMB as an antiseptic therapeutic agent is, however, impeded by its inherent cytotoxicity.

In previous investigations we have characterized the LPS-PMB interaction thermodynamically (12–14) by taking ''normal'' enterobacterial LPS from bacteria sensitive to the action of PMB. It was found, among others, in isothermal titration calorimetric (ITC) measurements that binding of PMB to enterobacterial LPS is entropically governed in the gel phase of the acyl chains of LPS ($<30°C$) but enthalpically driven in the liquid crystalline phase ($>35°C$) (14).

Differential scanning calorimetry (DSC) measurements were used to investigate the phase behavior of LPSRe in the presence of PMB. At low PMB contents (PMB/LPS ≥ 0.2 mol/mol) the presence of the peptide induced a broadening of the coexistence range. At higher PMB content (PMB/LPS molar ratios $> 0.8:1$), no phase transition was observed in the temperature range between 5–95°C, indicating a complete fluidization of the hydrocarbon chains. At this concentration ratio, the amount of negatively charged LPSRe and positively charged PMB cause an overall charge neutralization (14,15).

Submitted August 22, 2006, and accepted for publication December 4, 2006.

Address reprint requests to Klaus Brandenburg, Forschungszentrum Borstel, Div. of Biophysics Parkallee 10, D-23845 Borstel, Germany. Tel.: 49-(0)4537-188235; Fax: 49-(0)4537-188632; E-mail: Kbranden@fz-borstel.de.

0006-3495/07/04/2796/10 $2.00

doi: 10.1529/biophysj.106.095711

Here, we have extended these measurements to LPS from PMB-resistant strains, i.e., to deep rough mutant LPS Re (strain R45) from *P. mirabilis* and LPS from *B. abortus*. The ITC measurements allow us to clearly differentiate the binding behavior of these LPS to PMB from that of ''normal'' LPS from PMB-sensitive enterobacterial strains: Above the phase transition temperatures, T_m, binding is still endothermic (i.e., entropically driven), whereas that of enterobacterial LPS to PMB is exothermic due to the dominance of the electrostatic attraction between the negative charges of LPS and positive charges of the peptide. We have furthermore investigated the gel to liquid crystalline phase behavior and the aggregate structure of the various LPS in the presence of different amounts of PMB by DSC, Fourier transform infrared spectroscopy (FTIR), and synchrotron radiation x-ray diffraction and have again found specific differences between the LPS from PMB-sensitive and -resistant bacterial strains. A thermodynamic characterization of the PMB:LPS binding for different LPS, originating from bacteria sensitive to and resistant against PMB, is thus possible, which should also be valid for other CAMP.

MATERIALS AND METHODS

LPS and lipids

LPSs from deep rough mutant strains Re from *Salmonella minnesota* R595 (PMB sensitive) and *P. mirabilis* R45 (PMB resistant) were extracted from bacteria grown at 37°C by the phenol/chloroform/petrol ether method (16) and smooth form LPS from *B. abortus* by the phenol:water technique (2). LPS samples were purified, lyophilized, and used in their natural salt form. PMB was from Sigma (Deisenhofen, Germany). The smooth LPS of its *Ba*ΔlpcC mutant was prepared likewise.

The known chemical structures of LPS R595 and LPS R45 (3) are illustrated in Fig. 1. These natural samples are very heterogeneous, and LPS R45 differs from LPS R595 essentially by the presence of a L-arabinose at the first 2-keto-3-deoxyoctonate monosaccharide.

The structure of the *B. abortus* S-LPS is partly known (for a review, see Iriarte et al. (17)). The O-polysaccharide is a homopolymer of *N*-formylperosamine in α (1–2), and the core oligosaccharide is known to contain

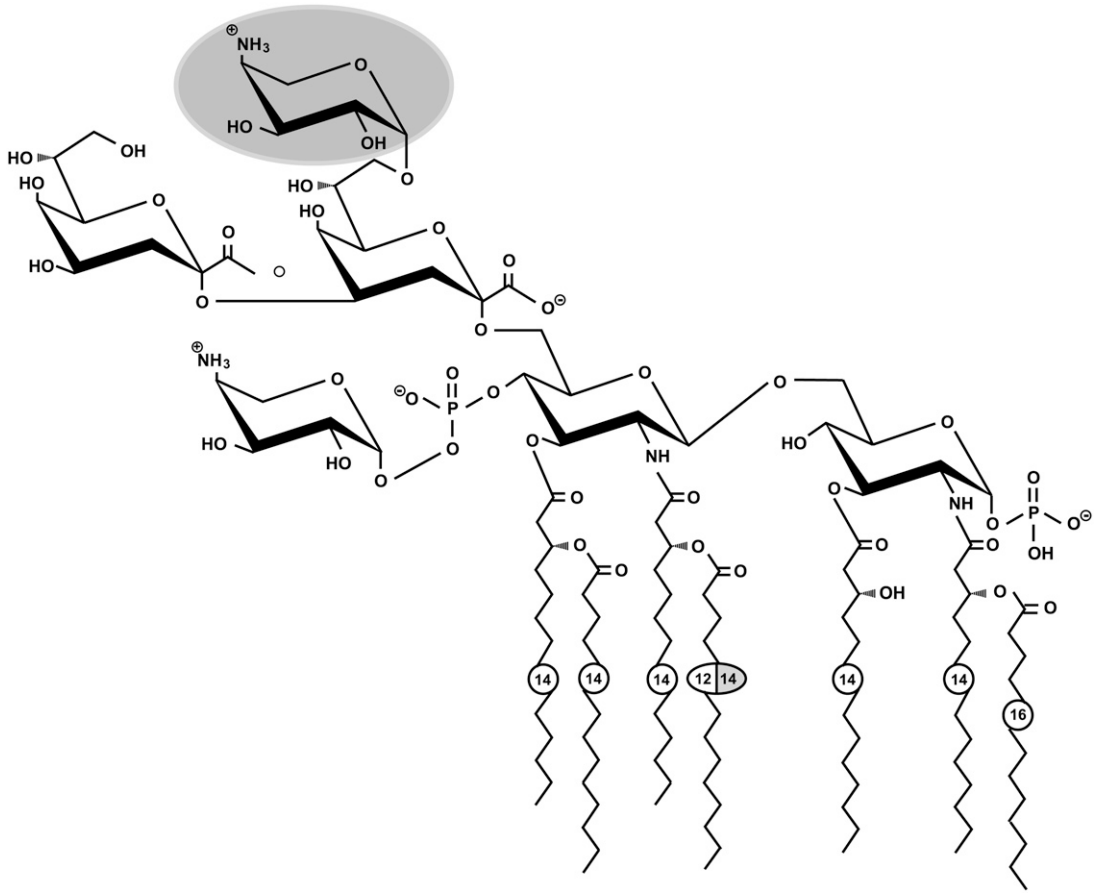

FIGURE 1 Chemical structures of LPSs from sensitive (*S. minnesota* R595) and resistant (*P. mirabilis* R45) strains according to Wiese et al. (3). Both LPS have nonstoichiometric substituents (acyloxyacyl chain C-16 in position 2 of the glucosamine I, amino-arabinose linked to the 4′-phosphate of glucosamine II). LPS R45 has a nonstoichiometric (~50%) substitution of an amino-arabinose (*dark label*), which leads to a reduction of the negative net charge as compared to LPS R595. Furthermore, the amide-bound acyl chain in position 2′ consists of a C-14 rather than a C-12 chain. Measured charges are −3.4 for LPS R595 and −3.0 for LPS R45 (3).

quinovosamine, glucose, glucosamine, mannose, and 3-deoxy-D-manno-2-octulosonic acid (Kdo). It lacks phosphate or acidic sugars other than Kdo. The structure of the LPS of mutant *Ba*ΔlpcC (PMB sensitive) is similar to that of the wild-type *B. abortus* (PMB resistant) but for a core defect. This mutant is deficient in the glycosyl transferase presumed to incorporate mannose into the inner core but despite this defect keeps an intact O-polysaccharide. The *Brucella* lipid A is a diaminoglucose disaccharide carrying very long chain fatty acids (up to 32 carbons long) in acyl-oxyacyl linkages. Resistance to PMB in *B. abortus* is attributed to the structure of the core oligosaccharide and the peculiar lipid A (2) but not to phosphate content, which is the same for the two LPS.

Sample preparation

The lipid samples were usually prepared as aqueous dispersions at high buffer (20 mM HEPES pH 7.0) content, depending on the sensitivity of the technique: 0.05–0.15 mM for the ITC experiments, 0.4 mM for the DSC experiments, and 20 mM for the FTIR and x-ray experiments. In all cases, the lipids were suspended directly in buffer, sonicated, and temperature cycled several times between 5°C and 70°C and then stored at least 12 h at 4°C before measurement.

Isothermal titration calorimetry

Microcalorimetric measurements of peptide binding to endotoxins were performed on a MCS isothermal titration calorimeter (MicroCal, Northampton, MA) at various temperatures. The endotoxin samples at a concentration of 0.05–0.15 mM—prepared as described above—were filled into the microcalorimetric cell (volume 1.3 ml) and the peptide in the concentration range 0.5–5 mM into the syringe (volume 100 μl), each after thorough degassing of the suspensions. After thermal equilibration, aliquots of 3 μl of peptide solution were injected every 5 min into the lipid-containing cell, which was stirred constantly, and the heat of interaction after each injection measured by the ITC instrument was plotted versus time. The total heat signal from each experiment was determined as the area under the individual peaks and plotted versus the [peptide]/[lipid] molar ratio. Since the instrument works in temperature equilibrium at a constant ''current feedback'' corresponding to a power of ~74 μW, an exothermic reaction leads to a lowering of this current and an endothermic reaction to an increase. All titrations, performed at constant temperatures, were repeated at least two times.

As control for the ITC experiments, PMB was titrated into pure buffer; however, only a negligible enthalpic reaction due to dilution could be observed (data not shown).

Fourier transform infrared spectroscopy

The infrared spectroscopic measurements were performed on an IFS-55 spectrometer (Bruker, Karlsruhe, Germany). The lipid samples were placed in a CaF_2 cuvette with a 12.5-μm Teflon spacer. Temperature scans were performed automatically between 10°C and 70°C with a heating rate of 0.6°C/min. Every 3°C, 50 interferograms were accumulated, apodized, Fourier transformed, and converted to absorbance spectra. For strong absorption bands, the band parameters (peak position, bandwidth, and intensity) were evaluated from the original spectra, if necessary after subtraction of the strong water bands.

Differential scanning calorimetry

DSC measurements were performed with a MicroCal VP scanning calorimeter (MicroCal). The heating and cooling rates were 1°C/min. Heating and cooling curves were measured in the temperature interval from 10°C to 100°C. The phase transition enthalpy was obtained by integration of the heat capacity curve as described previously (18). Usually, three consecutive heating and cooling scans were measured (19). The lipid dispersion was prepared according to recently described protocols at a concentration of ~1 mg/ml (corresponding to 0.4 mM) in phosphate buffer saline at pH 7.4 (20).

X-ray diffraction

X-ray diffraction measurements were performed at the European Molecular Biology Laboratory outstation at the Hamburg synchrotron radiation facility HASYLAB using the small angle x-ray scattering camera X33 (21). Diffraction patterns in the range of the scattering vector $0.1 < s < 1.0\ \mathrm{nm}^{-1}$ ($s = 2 \sin\theta/\lambda$, 2θ scattering angle, and λ the wavelength = 0.15 nm) were recorded at various temperatures with exposure times of 1 min using a linear detector with delay line readout (22). The s axis was calibrated with Ag-behenate, which has a periodicity of 58.4 nm. The diffraction patterns were evaluated as described previously (23), assigning the spacing ratios of the main scattering maxima to defined three-dimensional structures. Lamellar structures are most relevant here. They are characterized by reflections grouped in equidistant ratios, i.e., 1, 1/2, 1/3, 1/4, etc., of the lamellar repeat distance d_l.

RESULTS

Binding measurements

It has been shown recently that the interaction of PMB with enterobacterial rough mutant LPS from PMB-sensitive strains is endothermic in the gel phase (below 35°C) and exothermic in the liquid crystalline phase (>35°C) (14). ITC experiments were performed at 37°C with LPS from the PMB-resistant strains R45 and compared with LPS from the PMB-sensitive strain R595 (Fig. 2). For this, 3 μl of a 3 mM PMB solution were titrated into a 0.05 mM LPS dispersion every 5 min, and the calorimetric signals were recorded. Clearly, for LPS R595 the peaks directed downward (Fig. 2) are characteristic for an exothermic process, whereas for LPS R45 the upward peaks are indicative of an endothermic process. Therefore, binding of LPS R45 to PMB was monitored at temperatures below and above the phase transition, i.e., in the range 25–50°C (Fig. 3). It can be seen that the enthalpic change is always endothermic and is more or less constant at 25°C and 30°C in the gel phase. In the liquid crystalline phase at 40°C and 50°C, the ΔH-values at the beginning of the titration seem to decrease, but the basic course remains essentially the same. Thus, the comparison of these measurements with those for LPS from PMB-sensitive enterobacterial strains and also free lipid A, which exhibit exothermic binding isotherms at least in the liquid crystalline phase (14), indicate a different binding mechanism.

Phase transition measurements

FTIR was applied for the analysis of various functional groups of LPS from sensitive strain R595 and resistant strain R45 in the presence of PMB. As a sensitive measure of the state of order of the LPS acyl chains, the peak position of the symmetric stretching vibration of the methylene group $\nu_s(CH_2)$ was taken. In Fig. 4, the peak position of $\nu_s(CH_2)$ is plotted versus temperature for the LPS R595- and LPS R45-PMB complexes. For both samples, the phase transition temperature, T_m, lies at 30 –35°C; for LPS R595 (Fig. 4 *A*), it is drastically shifted to lower temperatures with increasing PMB concentration; for LPS R45 (Fig. 4 *B*), however, essentially a fluidization takes place in particular in the gel

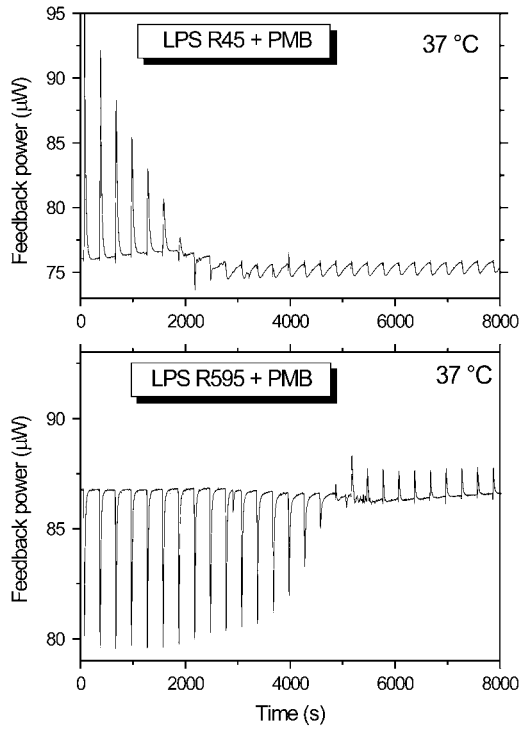

FIGURE 2 Isothermal calorimetric titration of LPS (0.05 mM) from *P. mirabilis* R45 (*top*) and *S. minnesota* R595 (*bottom*) with PMB (3 mM) at 37°C. The LPS dispersion in the calorimetric cell was titrated every 5 min with 3 μl of PMB. The increase in the feedback power indicates an endothermic, the decrease an exothermic process.

phase, which should result from the *trans-gauche* isomerization of the hydrocarbon chains.

Also DSC was applied for the elucidation of the chain melting process (Fig. 5). The data clearly show a sharp endothermic phase transition for the two LPS, with a phase transition enthalpy change ΔH_m much larger for LPS R595 (39 kJ/mol) than for LPS R45 (20 kJ/mol, see Table 1). With increasing PMB concentrations, the ΔH_m-values decrease and there is a concomitant broadening of the peaks, particularly at the onset of the acyl chain melting, which parallels the infrared observations. For LPS R45, the endothermic peak disappears at [LPS]/[PMB] = 1:0.4, whereas for LPS R595 two very small endotherms are seen even at [LPS]/[PMB] = 1:0.8. The broad transitions detectable in the infrared measurements at [LPS]/[PMB] = 1:1 are no longer detectable calorimetrically, indicating that a), the acyl chains of the lipid do not undergo a phase transition in the temperature range 5–95°C, or b), the process of chain melting occurring over this broad range is not resolvable by DSC.

LPS headgroup conformation

Infrared (IR) spectra of the LPS backbone, comprising the phosphate and sugar vibrational bands, were recorded in the absence and presence of an equimolar amount of PMB for LPS R595 and LPS R45 (Figs. 6 and 7). The bands around 1260 and 1220 cm^{-1} can be assigned to modes of the antisymmetric stretching vibration of the phosphate groups $\nu_{as}(PO_2^-)$, the bands at 1160–1170 cm^{-1} to glucosamine ring modes, and the two bands in the range –1090 cm^{-1} to unspecific sugar ring modes (24). The spectra for LPS R595 (Fig. 6) clearly show that there are considerable changes of the phosphate as well as the sugar modes. Regarding the phosphates, a drastic decrease of the band intensities at 1257 and 1221 cm^{-1} takes place; the former corresponds to phosphate with low hydration, mainly due to the 4′-phosphate, and the latter band to phosphate with high hydration, mainly due to the 1-phosphate. (25). The decrease of the intensities can be attributed to a strong reduction of the mobility of both phosphate groups. In contrast, the intensities of the phosphate bands of LPS R45 are only slightly reduced in the presence of PMB (Fig. 7). Similarly, for LPS R595 considerable band shifts are observed for the two sugar bands at 1030–1040 cm^{-1} and at 1070–1090 cm^{-1} with a large decrease of the wavenumber value for the first band and a complete disappearance and/or shift to higher wavenumbers for the second (Fig. 6). In contrast, again, the spectra of LPS R45 do not change much in the presence of PMB (Fig. 7), indicating only low affinity binding.

Aggregate structures of LPS

The aggregate structures of both LPS were investigated in the absence and presence of PMB using synchrotron radiation x-ray small-angle diffraction. In Fig. 8, the logarithm of the scattering intensity is plotted versus scattering vector $s = (2 \sin \theta/\lambda)$ for both LPS in the absence and presence of an equimolar amount of PMB. The diffraction patterns of both LPS in the absence of PMB exhibit a broad maximum between $s = 0.1$ and 0.35/nm, which can be assigned mainly to a unilamellar structure. However, the occurrence of a broad maximum between 0.4 and 0.55 nm indicates a second order, which might result from more than one bilayer. Additionally, small and sharp peaks are superimposed, which might be indicative of a cubic phase, as previously reported (26), but cannot be assigned unequivocally. In the presence of PMB, the figure changes drastically leading in both cases to the appearance of reflections at equidistant ratios typical for a multilamellar phase. The sharper diffraction peaks for LPS R45 should be due to a higher number of lamellae, but the peak positions lying at similar values indicate an overall similar structural preference. From these data, there is no basic difference in the aggregate structures, and thus no explanation of the differences in the ITC data can be derived from the supramolecular structures with respect to the thermodynamic differences as observed by ITC.

Investigations into Brucella LPS

For a test on the general validity of our findings, taxonomically distant bacteria with differences in the PMB sensitivity

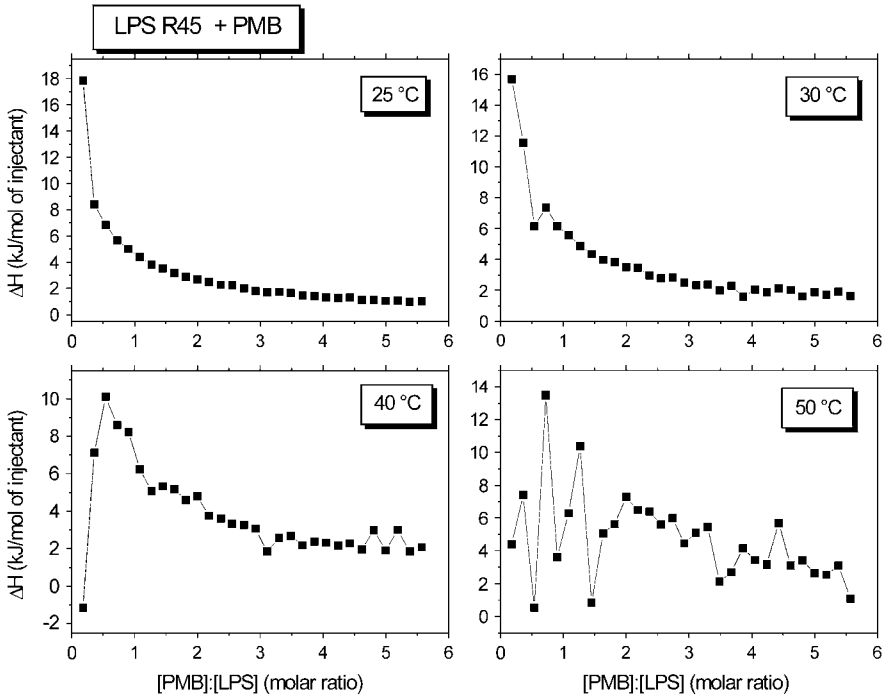

FIGURE 3 Enthalpy change of the LPS R45: PMB reaction versus [PMB]/[LPS] molar ratio between 25°C and 50°C, indicating exclusively endothermic reactions.

were investigated. For this, we have taken the PMB-sensitive and -resistant α-*Proteobacteria B. abortus* (*B.a.*). The wild-type strain 2308 is PMB resistant, whereas its *Ba*ΔlpcC mutant is PMB sensitive. The phase transition behavior was analyzed by FTIR and DSC to study the temperature range of their phases and the influence of PMB on it. In Figs. 9 and 10, the results are plotted for the two *B. abortus* LPS. Interestingly, these two LPS differed considerably in T_m, lying at >50°C for the mutant but ~30–35°C for the wild-type LPS. In the presence of PMB, for the LPS from the sensitive *Ba*ΔlpcC mutant (Figs. 9 *A* and 10 *A*) a drastic decrease of T_m takes place, whereas for wild-type 2308 LPS (Figs. 9 *B* and 10 *B*) an overall fluidization rather than a change in T_c is observed. This is in accordance with the

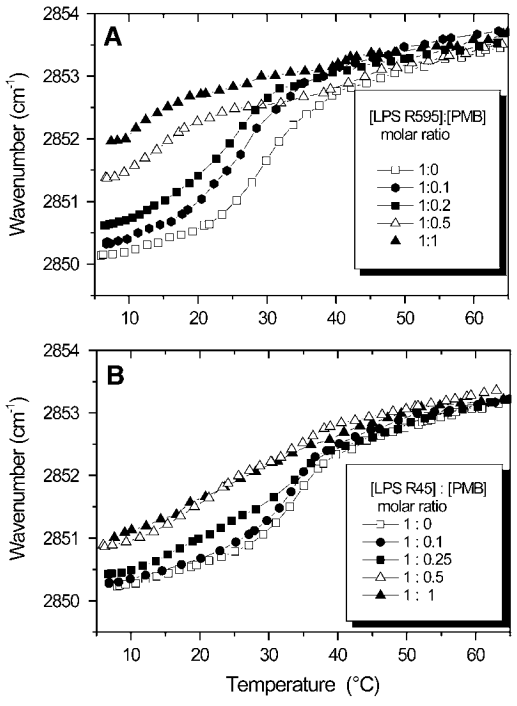

FIGURE 4 Gel to liquid crystalline ($\beta \leftrightarrow \alpha$) phase transition of the hydrocarbon chains of LPS R595 (*A*) and LPS R45 (*B*) at different PMB concentrations. The peak position of the symmetric stretching vibration of the methylene groups $\nu_s(CH_2)$ is plotted versus temperature.

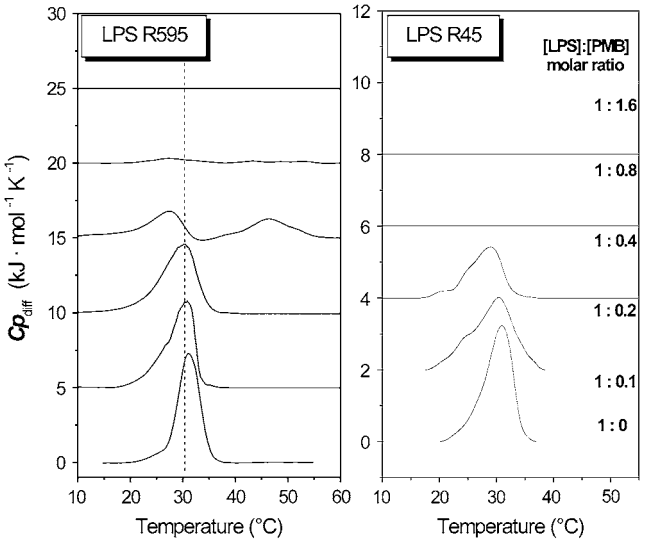

FIGURE 5 DSC heat capacity curves of mixtures of PMB with LPS R595 (*left column*) and R45 (*right column*) in various molar ratios. LPS concentrations were 1 mg/ml.

TABLE 1 Phase transition enthalpies ΔH (in kJ/mol) for the indicated LPS at various PMB molar ratios

LPS/PMB Mol/mol	LPS R595	LPS Re45	LPS 2308	LPS lpcC
1:0	39	20	12	11
1:0.1	37	18	10	10
1:0.2	36	11	8	7
1:0.4	15/12	0	0	4
1:0.8	4	0	0	0
1:1.6	0	0	0	0

calorimetric analysis of the heat capacity curves as a function of added peptide.

The enthalpy changes measured by DSC for *B. abortus* LPS are much lower than for the enterobacterial LPS (see Table 1), but the phase transitions disappear at similar [LPS]/[PMB] ratios in both cases. The lower phase transition enthalpy of LPS from *Ba*2308 and *Ba*ΔlpcC indicates reduced hydrophobic interactions between the hydrocarbon chains compared to, e.g., LPSR595.

In Figs. 11 and 12, we have summarized the results from ITC measurements at 25°C, 35°C, and 45°C. The LPS from *B. abortus* 2308 ($T_m \approx 32$°C) exhibits exclusively endotherms at all temperatures, with high ΔH-values during the first titrations at 25°C, which decrease at higher temperatures. Clearly, at [PMB]/[LPS 2308] $\geq$ 0.5, all curves are nearly identical. The behavior for the LPS of mutant *Ba*ΔlpcC from *B. abortus* is quite different. An endothermic reaction takes place in the gel and an exothermic reaction in the liquid crystalline phase corresponding to the behavior observed for enterobacterial LPS from PMB-sensitive strains. Furthermore, binding saturation takes place at a much higher [PMB]/[LPSlpcC] ratio than for the PMB-resistant LPS.

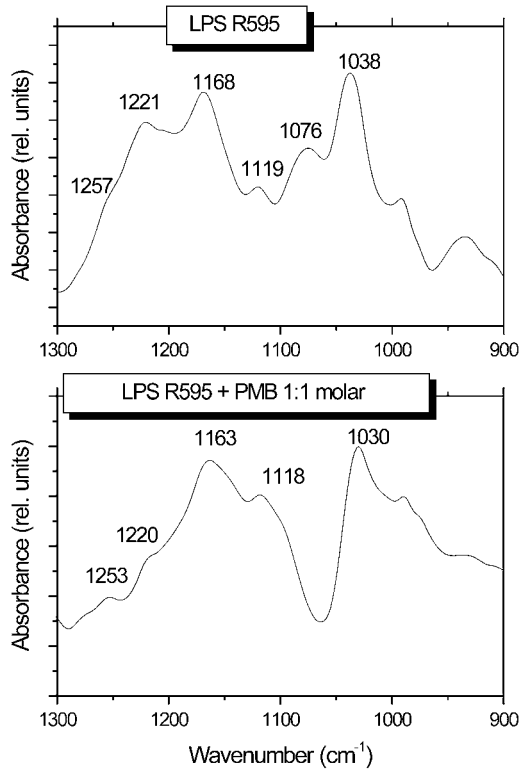

FIGURE 6 Infrared spectrum of LPS R595 in the region of phosphate and sugar vibrations in the absence (*top*) and presence (*bottom*) of an equimolar content of PMB. The band components at 1260–1220 cm^{-1} correspond to modes from the antisymmetric stretching vibration $\nu_{as}(PO_2^-)$, the band components 1178–1030 cm^{-1} to unspecific sugar ring vibrations (36).

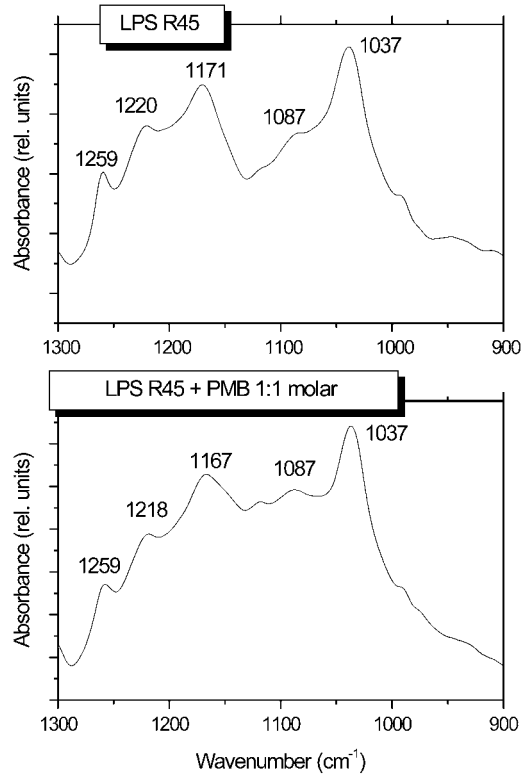

FIGURE 7 Infrared spectrum of LPS R45 in the region of phosphate and sugar vibrations in the absence (*top*) and presence (*bottom*) of an equimolar content of PMB.

IR spectra of the LPS backbone, comprising the phosphate and sugar vibrational bands, were recorded in the absence and presence of PMB for *Ba* 2308 and *Ba* ΔlpcC. As described above for the LPS R595 and R45, the two *Brucella* LPS exhibit completely different behavior: The resistant wild-type LPS 2308 display nearly no significant changes in the IR ''fingerprint'' region, whereas for the LPS mutant *Ba*ΔlpcC considerable changes of the IR spectra can be observed upon PMB binding (data not shown).

DISCUSSION

Bacterial resistance represents an increasingly threatening development in infectiology. In many cases the reasons for this can be attributed to chemical changes of the cell envelope of the microorganisms. In particular, since the outer

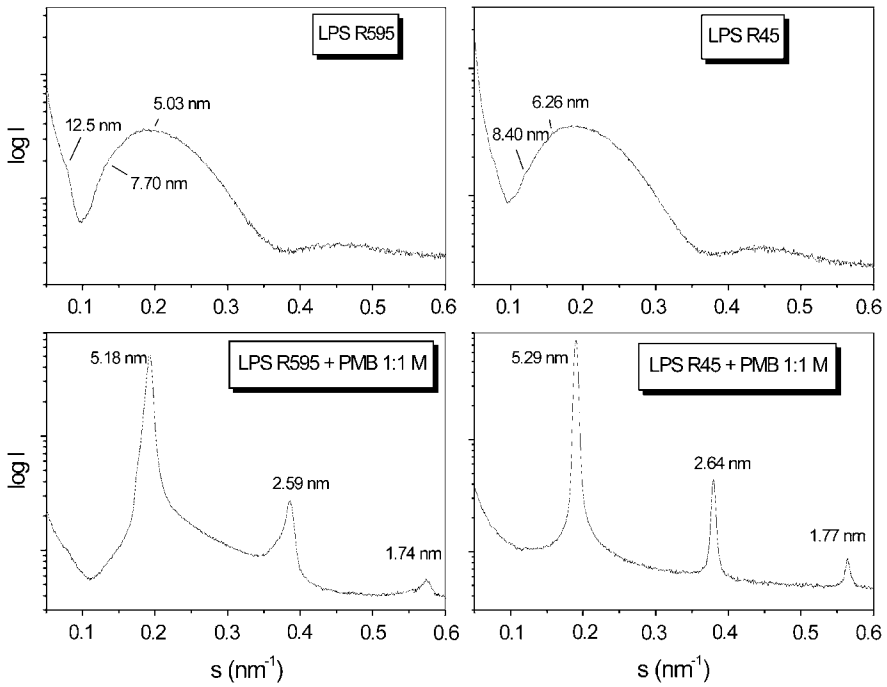

FIGURE 8 Synchrotron radiation small angle x-ray diffraction of LPS R595 and R45 alone (*top*) and in the presence of an equimolar content of PMB (*bottom*). The logarithm of the scattering intensity (log I) is plotted versus scattering vector $s = 1/d$ (d-spacings in nm).

leaflet of Gram-negative bacteria, consisting mainly of LPS, is the first point of attack for antibiotics and components of the immune system, bacteria may develop mutations in the chemical structure of LPS. Thus, lipid A modifications as well as changes in the efflux pump have been observed to cause CAMP resistance in *Neisseria meningiditis* (27), arabinose and glycine substitution of LPS in serum- and PMB-resistant strains from *Yersinia pestis* (28), changes in LPS core and lipid A structure in CAMP-resistant *Brucella* spp. (1), and changes in lipid A and O-antigen structure in CAMP-resistant *P. mirabilis* mutants (29). Interestingly, changes in LPS chemical structure were also observed for combined quinolone and β-lactam resistance of *Pseudomonas aeruginosa* (30).

In most cases, the changes of the chemical structures responsible for AMP resistance are not known in detail. Only for some PMB-resistant enterobacteriaceae can the changes in the chemical structures be quantitated; in particular, 4-amino-deoxy-arabinose is an additional substituent in the lipid A and/or inner core oligosaccharide region of LPS (31,32), similar to recent findings with LPS R595 and LPS R45 (3) (see Fig. 1). In the last case the PMB sensitivity and resistance of the bacteria were interpreted on the basis of investigations of an asymmetric phospholipid/LPS planar membrane mimicking the outer membrane of the bacteria. It was found that the self-promoted transport of PMB through the membrane directly correlated with the surface charge density of the LPS layer: In the PMB-sensitive strain with high negative charge density, PMB induced transient membrane lesions with diameters large enough ($d = 2.4$ nm) for permeation of PMB. For PMB-resistant strains, lesions too small to be permeated by PMB were observed, most likely because the negative charge density was significantly lower. Thus, the decisive parameter determining PMB resistance seems to be additional positive charges in the headgroup region of LPS (Fig. 1). In particular, the additional arabinose in Fig. 1 is apparently a determinant of PMB resistance by lowering the negative charge at the membrane surface and representing a sterical disturbance for the attack of PMB.

For the PMB-resistant and -sensitive strains from *B. abortus*, the precise details of the chemical structures of the LPS are unknown. However, both chemical and genetic analyses as well as comparative genomics strongly suggest a structure for the core oligosaccharide in which mannose linked to KdoI is the first sugar in a lateral branch that protects acidic residues from binding by polycations (17). Thus, the mutant *Ba*ΔlpcC, which lacks the putative mannosyl transferase, carries a severe defect in this branch and at the same time an intact O-polysaccharide. With respect to phosphate contents, there are no differences between the two LPSs. Although they remain to be confirmed by precise structural analysis, these data are consistent with the observations presented here on the increased PMB binding of *Ba*ΔlpcC.

We have found that the temperature dependence of the PMB binding measured with ITC exhibited considerable differences between LPS from resistant and sensitive strains: In the liquid crystalline phase, for LPS from PMB-sensitive strains the data clearly indicate an exothermic reaction (Fig. 2, *bottom*), in accordance with previous work for other endotoxins, lipid A, and LPS with moderately long sugar chains lengths (LPS Re to Rc) (14). For other LPS with longer sugar chains (LPS Ra and S-form), exothermic reactions are even partially found in the gel phase. In contrast to this, LPS from

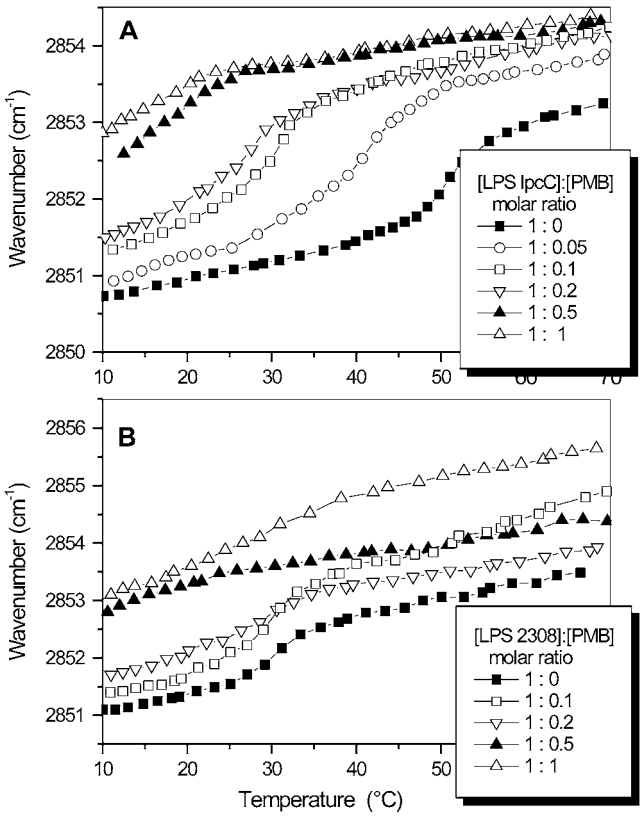

FIGURE 9 Gel to liquid crystalline ($\beta \leftrightarrow \alpha$) phase transition of the hydrocarbon chains of LPS B.a. lpcC (*A*) and LPS B.a.2308 (*B*) at different PMB concentrations. The peak position of the symmetric stretching vibration of the methylene groups $\nu_s(CH_2)$ is plotted versus temperature.

PMB-resistant strains displays only endothermic reactions in both phases (Figs. 3 and 11). This means that the entropically governed reaction of PMB with the hydrophilic headgroup, including the ordered water layer around the backbone as observed in the gel phase, perpetuates in the liquid crystalline phase. Thus, the electrostatic attraction between the positive charges of PMB and the negative charges of LPS, resulting in an exothermic process, is superimposed by the interaction of PMB with ordered water and counterion layers, which are decomposed in an endothermic reaction. This endothermic enthalpy change in the LPS backbone exceeds the exothermic enthalpy change of the charge attraction, resulting in a net endothermic process. Concomitantly with these data, the phase transition behavior in the presence of PMB is characteristically different for LPS from sensitive and resistant strains. For LPS from sensitive strains (LPS R595 and LPS BaΔlpcC, Figs. 4 *A* and 9 *A*), the phase transition temperatures decrease considerably, in contrast with the situation with LPS from resistant strains (LPS R45 and LPS Ba2308, Figs. 4 *B* and 9 *B*), where the decrease in T_m is replaced by a ''smearing'' of the phase transition over a wide temperature.

It has to be emphasized that the two effects superimpose, as can be deduced from a comparison of Figs. 9, 11, and 12,

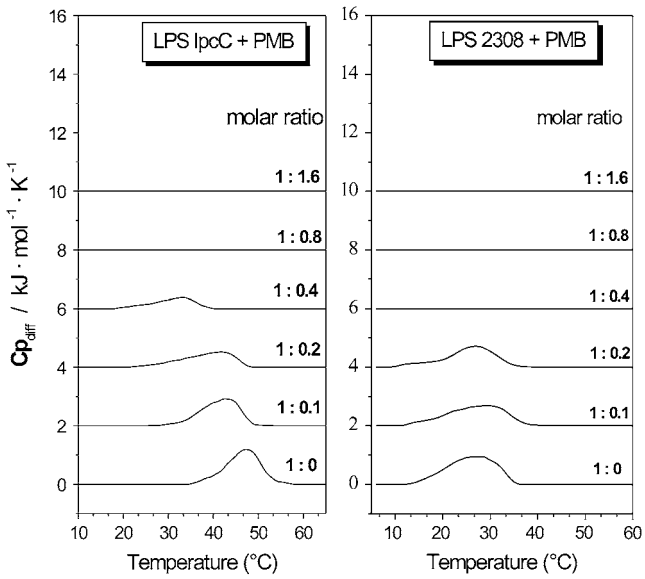

FIGURE 10 DSC heat capacity curves of mixtures of PMB with LPS lpcC (*left column*) and LPS. 2308 (*right column*) in various molar ratios. LPS concentrations were 1 mg/ml.

and LPS 2308/PMB becomes highly fluid at a 1:0.5 molar ratio at all temperatures (Fig. 9 *B*), but the reaction in the ITC remains always endothermic (Fig. 11). Vice versa, LPS lpcC/PMB at a 1:0.5 molar ratio is fluid also at all temperatures (Fig. 9 *A*), but nevertheless the reaction remains endothermic at 25°C and 35°C and becomes exothermic at higher temperatures (Fig. 12). This last finding means that the conversion endothermic-exothermic is decoupled from the phases of the acyl chains. The high phase transition temperature (>50°C, Figs. 9 *A* and 10) is particularly noteworthy. For other bacteria it has never been observed that LPS as the

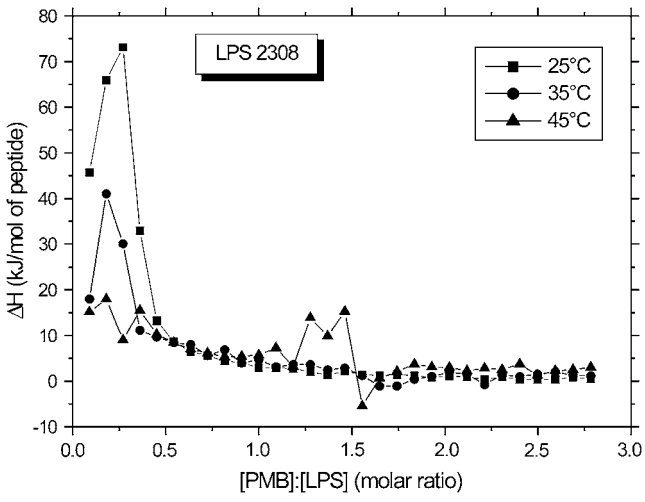

FIGURE 11 Enthalpy change of the LPS 2308/PMB reaction versus [PMB]/[LPS] molar ratio between 25°C and 45°C, indicating exclusively endothermic reactions.

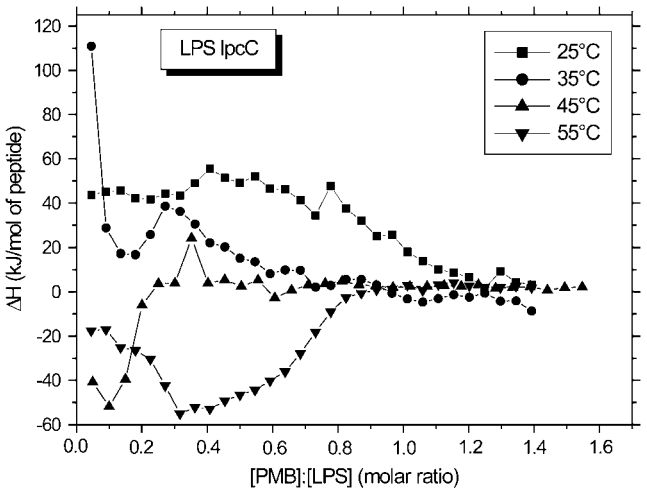

FIGURE 12 Enthalpy change of the LPS lpcC:PMB reaction versus [PMB]/[LPS] molar ratio between 25°C and 55°C, indicating endothermic reactions at 25°C and 35°C and exothermic reactions above.

main component of the outer membrane is so rigid at 37°C also in isolated form (wavenumbers at 2851 cm^{-1} correspond nearly to the gel phase). This may be understood by assuming that LPS within the outer membrane interacts with, e.g., membrane proteins, in a way that the acyl chain fluidity is increased, as observed for OmpT and PhoE (33,34).

The infrared spectra of the headgroup region (Figs. 6 and 7) provide a more precise characterization of the interaction: The bands from the phosphate and sugar parts of the PMB-sensitive strain (R595) are strongly affected by the PMB binding (Fig. 6); in particular the drastic intensity decrease of the two phosphate bands at 1220–1260 cm^{-1} indicates a immobilization of these groups, and the shift or even disappearance of the bands at 1030–1076 cm^{-1} indicates that PMB binding also affects the sugars. In contrast, the headgroup region of LPS from the resistant strain is nearly unaffected by the presence of PMB (Fig. 7), indicating a lower accessibility of PMB to the phosphate groups. From this and the observation that the overall negative headgroup charge is only lowered from −3.4 for LPS R595 to −3.0 for LPS R45 (Fig. 1), it can be concluded that the steric changes due to the presence of the bulky amino-arabinose, rather than the change in negative charge density, are the most important factors for the expression of resistance to polycationic antimicrobial peptides.

Interestingly, despite the considerable differences between the two LPS chemotypes, the aggregation behavior in the absence as well as presence of PMB is quite similar (Fig. 8). Both LPS show a preference for a unilamellar structure, possibly superimposed by a nonlamellar fraction, in accordance with previous results (35). According to the data of Snyder et al. (36), who performed x-ray diffraction studies with LPS bilayers, a multilamellar structure with a low number of lamellae can also not be excluded, and the appearance of the broad ''second order maximum'' as described above (see Fig. 8) would support this view. We have, however, found in recent freeze-fracture electron microscopic experiments that the morphology of LPS R595 consists of a kind of ''open eggshells'' with no significant bilayer stacking at the surface (J. Howe, W. Richter, and K. Brandenburg, unpublished results). This rules out a high number of lamellae. In the presence of PMB, a multilamellar structure is clearly detected. The periodicities for both types of LPS in the presence of PMB lie around 5.20–5.30 nm and are thus significantly lower than the corresponding values (5.9–6.4 nm) found in conditions under which LPS Re adopts multilamellar structures (low water content or high Mg^{2+} concentration (37)). From this it can be deduced that PMB results in an attractive interbilayer interaction which lowers the thickness of the water layers between adjacent bilayers. The x-ray diffraction data imply, furthermore, that PMB causes a considerable reaggregation also of the LPS from the PMB-resistant strain R45, although the other presented data indicate that only weak interactions are involved.

It must be emphasized, however, that for the expression of bacterial resistance the LPS monolayer at the bacterial surface is the decisive epitope and that the details of the interaction of PMB with the LPS headgroup region as described above are more important than the aggregation behavior of isolated LPS. This behavior should, instead, play a role in the ability of CAMPs to inhibit the LPS-induced cytokine production in immune cells as described earlier (6,38).

We thank G. von Busse for performing the ITC and FTIR spectroscopic measurements and B. Fölting for DSC support.

The study has been carried out with financial support from the Commission of the European Communities, specific RTD program ''Quality of Life and Management of Living Resources'', QLCK2-CT-2002-01001, ''Antimicrobial endotoxin neutralizing peptides to combat infectious diseases''. Research at the Dept. of Microbiology of the University of Navarra is supported by Ministerio de Ciencia y Tecnología of Spain (Proyecto AGL2004-01162/GAN).

REFERENCES

1. Martinez de Tejada, G., J. Pizarro-Cerda, E. Moreno, and I. Moriyon. 1995. The outer membranes of *Brucella* spp. are resistant to bactericidal cationic peptides. *Infect. Immun.* 63:3054–3061.
2. Velasco, J., J. A. Bengoechea, K. Brandenburg, B. Lindner, U. Seydel, D. González, U. Zähringer, E. Moreno, and I. Moriyón. 2000. *Brucella abortus* and its closest phylogenetic relative, *Ochrobactrum* spp., differ in outer membrane permeability and cationic peptide resistance. *Infect. Immun.* 68:3210–3218.
3. Wiese, A., M. Münstermann, T. Gutsmann, B. Lindner, K. Kawahara, U. Zähringer, and U. Seydel. 1998. Molecular mechanisms of polymyxin B-membrane interactions: direct correlation between surface charge density and self-promoted uptake. *J. Membr. Biol.* 162:127–138.
4. Schromm, A. B., K. Brandenburg, H. Loppnow, A. P. Moran, M. H. J. Koch, E. Th. Rietschel, and U. Seydel. 2000. Biological activities of lipopolysaccharides are determined by the shape of their lipid A portion. *Eur. J. Biochem.* 267:2008–2013.
5. Bone, R. C. 1993. Gram-negative sepsis: a dilemma of modern medicine. *Clin. Microbiol. Rev.* 6:57–68.
6. Andrä, J., K. Lohner, S. E. Blondelle, R. Jerala, I. Moriyon, M. H. Koch, P. Garidel, and K. Brandenburg. 2005. Enhancement of

endotoxin neutralization by coupling of a C12-alkyl chain to a lactoferricin-derived peptide. *Biochem. J.* 385:135–143.

7. Blondelle, S. E., and R. A. Houghten. 1992. Design of model amphipathic peptides having potent antimicrobial activities. *Biochemistry.* 31:12688–12694.
8. Ganz, T., and R. I. Lehrer. 1998. Antimicrobial peptides of vertebrates. *Curr. Opin. Immunol.* 10:41–44.
9. Lehrer, R. I., and T. Ganz. 2002. Cathelicidins: a family of endogenous antimicrobial peptides. *Curr. Opin. Hematol.* 9:18–22.
10. Liechty, A., J. Chen, and M. K. Jain. 2000. Origin of antibacterial stasis by polymyxin B in *Escherichia coli*. *Biochim. Biophys. Acta.* 1463:55–64.
11. Benz, R. 1984. Structure and selectivity of porin channels. *Curr. Top. Membr. Transport.* 21:199–217.
12. Brandenburg, K., I. Moriyon, M. D. Arraiza, G. Lehwark-Yvetot, M. H. J. Koch, and U. Seydel. 2002. Biophysical investigations into the interaction of lipopolysaccharide with polymyxins. *Thermochim. Acta.* 382:189–198.
13. Brandenburg, K., M. D. Arraiza, G. Lehwark-Yvetot, I. Moriyon, and U. Zähringer. 2002. The interaction of rough and smooth form lipopolysaccharides with polymyxins as studied by titration calorimetry. *Thermochim. Acta.* 394:53–61.
14. Brandenburg, K., A. David, J. Howe, M. H. Koch, J. Andrä, and P. Garidel. 2005. Temperature dependence of the binding of endotoxins to the polycationic peptides polymyxin B and its nonapeptide. *Biophys. J.* 88:1845–1858.
15. Brandenburg, K., P. Garidel, J. Howe, J. Andrä, L. Hawkins, M. H. J. Koch, and U. Seydel. 2006. What can calorimetry tell us about changes of the three-dimensional aggregate structure of phospholipids and glycolipids? *Thermochim. Acta.* 445:133–143.
16. Galanos, C., O. Lüderitz, and O. Westphal. 1969. A new method for the extraction of R lipopolysaccharides. *Eur. J. Biochem.* 9:245–249.
17. Iriarte, M., D. Monreal, R. Conde, I. Lopez-Goni, J. J. Letesson, and I. Moriyon. 2004. *Brucella* lipopolysaccharide: structure, biosynthesis and genetics. *In Brucella*: Molecular and Cellular Biology. I. Lopez-Goni and I. Moriyon, editors. Horizon Bioscience, Wymondham, UK. 159–192.
18. Blume, A., and P. Garidel. 1999. Lipid model membranes and biomembranes. *In* From Macromolecules to Man. R. B. Kemp, editor. Elsevier, Amsterdam. 109–173.
19. Garidel, P., and A. Blume. 2000. Interaction of alkaline earth cations with the negatively charged phospholipid 1,2-dimyristoyl-*sn*-glycero-3-phosphoglycerol. *Biophys. Biochem. Acta.* 1466:245–259.
20. Garidel, P., M. Rappolt, A. B. Schromm, J. Howe, K. Lohner, J. Andrä, M. H. Koch, and K. Brandenburg. 2005. Divalent cations affect chain mobility and aggregate structure of lipopolysaccharide from *Salmonella minnesota* reflected in a decrease of its biological activity. *Biochim. Biophys. Acta.* 1715:122–131.
21. Koch, M. H. J. 1988. Instruments and methods for small-angle scattering with synchrotron radiation. *Makromol. Chem. Macromol. Symp.* 15: 79–90.
22. Boulin, C., R. Kempf, M. H. J. Koch, and S. M. McLaughlin. 1986. Data appraisal, evaluation and display for synchrotron radiation experiments: hardware and software. *Nucl. Instr. Meth.* A249:399–407.
23. Brandenburg, K., W. Richter, M. H. J. Koch, H. W. Meyer, and U. Seydel. 1998. Characterization of the nonlamellar cubic and H_{II} structures of lipid A from *Salmonella enterica* serovar Minnesota by x-ray diffraction and freeze-fracture electron microscopy. *Chem. Phys. Lipids.* 91:53–69.
24. Brandenburg, K., and U. Seydel. 1998. Infrared spectroscopy of glycolipids. *Chem. Phys. Lipids.* 96:23–40.
25. Brandenburg, K., S. Kusumoto, and U. Seydel. 1997. Conformational studies of synthetic lipid A analogues and partial structures by infrared spectroscopy. *Biochim. Biophys. Acta.* 1329:193–201.
26. Brandenburg, K., M. Matsuura, H. Heine, M. Müller, M. Kiso, H. Ishida, M. H. J. Koch, and U. Seydel. 2002. Biophysical characterization of triacyl monosaccharide lipid A partial structures in relation to bioactivity. *Biophys. J.* 83:322–333.
27. Tzeng, Y. L., K. D. Ambrose, S. Zughaier, X. Zhou, Y. K. Miller, W. M. Shafer, and D. S. Stephens. 2005. Cationic antimicrobial peptide resistance in *Neisseria meningitidis*. *J. Bacteriol.* 187:5387–5396.
28. Anisimov, A. P., S. V. Dentovskaya, G. M. Titareva, I. V. Bakhteeva, R. Z. Shaikhutdinova, S. V. Balakhonov, B. Lindner, N. A. Kocharova, S. N. Senchenkova, O. Holst, G. B. Pier, and Y. A. Knirel. 2005. Intraspecies and temperature-dependent variations in susceptibility of *Yersinia pestis* to the bactericidal action of serum and to polymyxin B. *Infect. Immun.* 73:7324–7331.
29. McCoy, A. J., H. Liu, T. J. Falla, and J. S. Gunn. 2001. Identification of *Proteus mirabilis* mutants with increased sensitivity to antimicrobial peptides. *Antimicrob. Agents Chemother.* 45:2030–2037.
30. Leying, H. J., K. H. Buscher, W. Cullmann, and R. L. Then. 1992. Lipopolysaccharide alterations responsible for combined quinolone and beta-lactam resistance in *Pseudomonas aeruginosa*. *Chemotherapy.* 38: 82–91.
31. Nummila, K., I. Kilpeläinen, U. Zähringer, M. Vaara, and I. M. Helander. 1995. Lipopolysaccharides of polymyxin B-resistant mutants of *Escherichia coli* are extensively substituted by 2-aminoethyl pyrophosphate and contain aminoarabinose in lipid A. *Mol. Microbiol.* 16:271–278.
32. Boll, M., J. Radziejewska-Lebrecht, C. Warth, D. Krajewska-Pietrasik, and H. Mayer. 1994. 4-Amino-4-deoxy-L-arabinose in LPS of enterobacterial R-mutants and its possible role for their polymyxin reactivity. *FEMS Immunol. Med. Microbiol.* 8:329–342.
33. Andrä, J., H. de Cock, P. Garidel, J. Howe, A. B. Schromm, and K. Brandenburg. 2005. Investigation into the interaction of the phosphoporin PhoE with outer membrane lipids: physicochemical characterization and biological activity. *Medicinal Chem.* 1:537–546.
34. Brandenburg, K., P. Garidel, A. B. Schromm, J. Andrä, A. Kramer, M. Egmond, and A. Wiese. 2005. Investigation into the interaction of the bacterial protease OmpT with outer membrane lipids and biological activity of OmpT: lipopolysaccharide complexes. *Eur. Biophys. J.* 34:28–41.
35. Seydel, U., M. H. J. Koch, and K. Brandenburg. 1993. Structural polymorphisms of rough mutant lipopolysaccharides Rd to Ra from *Salmonella minnesota*. *J. Struct. Biol.* 110:232–243.
36. Snyder, S., D. Kim, and T. J. McIntosh. 1999. Lipopolysaccharide bilayer structure: effect of chemotype, core mutations, and temperature. *Biochemistry.* 38:10758–10767.
37. Brandenburg, K., M. H. J. Koch, and U. Seydel. 1992. Phase diagram of deep rough mutant lipopolysaccharide from *Salmonella minnesota* R595. *J. Struct. Biol.* 108:93–106.
38. Andrä, J., M. Lamata, G. Martinez de Tejada, R. Bartels, M. H. J. Koch, and K. Brandenburg. 2004. Cyclic antimicrobial peptides based on *Limulus* anti-lipopolysaccharide factor for neutralization of lipopolysaccharide. *Biochem. Pharmacol.* 68:1297–1307.